International Journal of Pharmaceutics 418 (2011) 254–264

Contents lists available at ScienceDirect

International Journal of Pharmaceutics

journal homepage: www.elsevier.com/locate/ijpharm

A priori performance prediction in pharmaceutical wet granulation: Testing the applicability of the nucleation regime map to a formulation with a broad size distribution and dry binder addition

Defne Kayrak-Talay[a], James D. Litster[a,b,*]

[a] School of Chemical Engineering, Purdue University, West Lafayette, IN 47907, USA
[b] Department of Industrial and Physical Pharmacy, Purdue University, West Lafayette, IN 47907, USA

ARTICLE INFO

Article history:
Received 6 December 2010
Received in revised form 24 March 2011
Accepted 8 April 2011
Available online 16 April 2011

Keywords:
Wet granulation
Quality by design
Gabapentin
Wetting and nucleation
Regime map

ABSTRACT

In this study, Hapgood's nucleation regime map (Hapgood et al., 2003) was tested for a formulation that consists of an active pharmaceutical ingredient (API) of broad size distribution and a fine dry binder. Gabapentin was used as the API and hydroxypropyl cellulose (HPC) as the dry binder with deionized water as the liquid binder. The formulation was granulated in a 6 l Diosna high shear granulator. The effect of liquid addition method (spray, dripping), liquid addition rate (29–245 g/min), total liquid content (2, 4 and 10%), and impeller speed (250 and 500 rpm) on the granule size distribution and lump formation were investigated. Standard methods were successfully used to characterize the process parameters (spray drop size, spray geometry and powder surface velocity) for calculating the dimensionless spray flux. However, the addition of dry binder had a very strong effect on drop penetration time that could not be predicted from simple capillary flow considerations. This is most likely due to preferential liquid penetration into the fine pores related to the dry binder particles and subsequent partial softening and dissolution of the binder. For systems containing a dry binder or other amorphous powders, it is recommended that drop penetration time be measured directly for the blended formulation and then scaled to the drop size during spraying.

Using these approaches to characterize the key dimensionless groups (dimensionless spray flux and drop penetration time), Hapgood's nucleation regime map was successfully used to predict *a priori* the effect of process conditions on the quality of the granule size distribution as measured by lump formation and the span of the size distribution, both before and after wet massing for range of conditions studied. Wider granule size distributions and higher amount of lumps were obtained moving from intermediate to mechanical dispersion regime. Addition of the liquid in the dripping mode gave the broadest size distribution with ungranulated fines and highest percentage of lumps compared to spraying mode. Addition of the liquid by spraying in the intermediate regime gave the narrowest size distribution with the lowest amount of lumps. The effects of impeller speed and wet massing time on granule size distribution were complex. At 2% liquid content, increasing the impeller speed and adding wet massing time caused some breakage of lumps and the production of fines. At higher liquid contents, the effects were less clear, likely due to a balance between increased breakage and increased granule consolidation and growth. Nevertheless, this work has demonstrated that for complex formulations with dry binder addition, the final granule size distribution still depends strongly on the homogeneity of the initial liquid distribution which is well predicted by the nucleation regime map analysis.

1. Introduction

This study reports results from a larger case study on model-based design space development for solid dosage form manufacture across length scales with stability considerations. The formulation and the manufacturing sequence are fixed. Gabapentin as API and hydroxypropyl cellulose (HPC) as dry binder are used as granulation materials. The manufacturing line has several unit operations including granulation, fluid bed drying, blending and tableting.

In modeling all industrial solids processing, the aim is to relate the product attributes to process parameters and formulation properties to determine the operation window at all scales. There are different quantitative engineering approaches available based on the level of knowledge to optimize the process (see Table 1). If

* Corresponding author at: School of Chemical Engineering, Purdue University, 480 Stadium Mall Dr, West Lafayette, IN 47907, USA. Tel.: +1 765 496 2836, fax: +1 765 494 0805.
E-mail address: jlitster@purdue.edu (J.D. Litster).

0378-5173/$ – see front matter © 2011 Elsevier B.V. All rights reserved.
doi:10.1016/j.ijpharm.2011.04.019

Table 1
Quantitative engineering approaches for scale up and design.

What do we know?	How do we design experiments and scale?	Implications
Nothing except parameters we can vary	Statistical experimental design	Lots of experiments at all scales
Controlling mechanisms	Careful formulation and process characterization Designing experiments based on dimensionless groups and regime maps	Reduced experiments at all scales
Fully predictive model	Careful formulation and process characterization Design minimum number of experiments to validate and fine tune the model	Use dimensionless groups to scale up Least number of experiments Pilot/full scale model validation and parameter estimation

there is no mechanistic information about the process, except for the process parameters, then statistical experimental designs are used to determine the effects of process parameters on the product properties. The statistical experimental design approach requires many experiments at all scales, and all the relations developed are empirical and have little information to bridge across scales. A more desirable approach is to have fully predictive mathematical models covering all the physical phenomena taking place in the process. Then, the least number of experiments are required at all scales to validate the model and estimate the model parameters.

For high shear wet granulation, the complex nature of the process does not allow us to have fully predictive models at the moment. This is a current area of active research. A variety of modeling approaches are being developed towards developing true engineering design models based on different mathematical frameworks including on population balance modeling, (Adetayo and Ennis, 1997; Biggs et al., 2003; Hounslow et al., 2001; Iveson, 2002; Poon et al., 2008; Ramachandran et al., 2009; Verkoeijin et al., 2002), and coupled DEM-population balance modeling (Freireich et al., in press; Gantt and Gatzke, 2005).

The regime map approach falls in between statistical experimental design method and full predictive mathematical models in terms of level scrutiny and also number of experiments that need to be performed (Table 1). In this approach, key dimensionless groups which control different aspects of the process physics are defined. Process and formulation parameters are chosen to place the process in the desired regime of operation. Scale up is performed keeping all key dimensionless groups constant if possible.

The processes occurring in high shear wet granulation are categorized as wetting and nucleation, consolidation and growth, and breakage and attrition. Dimensionless groups and regime maps have been developed for growth and consolidation (Iveson et al., 2001; Iveson and Litster, 1998). The key dimensionless groups which define the regime of operation on growth regime map are maximum liquid saturation (S_{max}) and Stokes deformation number (St_{def}) (Iveson et al., 2001). Dimensionless spray flux (ψ_a) and dimensionless penetration time (τ_p) define operation regime on the nucleation map (Hapgood et al., 2003). These four dimensionless groups are defined as:

$$\psi_a = \frac{3\dot{V}}{2\dot{A}d_d} \quad (1)$$

$$\tau_p = \frac{t_p}{t_c} \quad (2)$$

$$S_{max} = \frac{w\rho_s(1-\varepsilon_{min})}{\rho_l\varepsilon_{min}} \quad (3)$$

$$St_{def} = \frac{\rho_g {U_c}^2}{2Y_d} \quad (4)$$

where $\dot{V}$ is spray flux, $\dot{A}$ is powder flux, d_d is drop diameter, t_p is drop penetration time and t_c is the circulation time inside the granulator, w is the mass ratio of liquid to solid, ε_{min} the minimum porosity the formulation reaches for that particular set of operating conditions, ρ_s and ρ_l are the density of solid particles and the liquid density respectively, ρ_g is granule density, U_c is representative collision velocity, and Y_d is dynamic yield stress. There are fewer studies on wet granule breakage compared to two other processes. Tardos et al. (1997) introduced a criterion for breakage based on a version of the Stokes deformation number. If St_{def} exceeds a critical value then breakage occurs. Recent experimental studies have validated this approach, although slightly different definitions of St_{def} are used (Liu et al., 2009; Van den Dries et al., 2003).

An extensive literature on high shear wet granulation was reviewed by Kristensen and Schaefer (1987) and Gokhale et al. (2005). More recent experimental studies that investigated the effects of process conditions and formulation properties on the final granule properties were presented by Benali et al. (2009), Bouwman et al. (2005), Bouwman et al. (2006), Cantor et al. (2009), Ghorab and Adeyeye (2007), Le et al. (2011), Mackaplow et al. (2000), Mangwandi et al. (2010), Mangwandi et al. (2011), Michaels et al. (2009), Realpe and Velazquez (2008), and Smirani-Khayati et al. (2009). In most of these studies, the effects of process variables and formulation properties on growth behavior and granule properties were discussed considering how Stokes deformation number or the balance between coalescence and breakage would be affected by a change in any of the variables. Of these papers, Benali et al. (2009), Bouwman et al. (2005), Bouwman et al. (2006), and Michaels et al. (2009) specifically used dimensional numbers and regime map approach to analyze their data.

The regime map approach for nucleation and wetting has largely been validated in the literature with relatively simple single component crystalline powder systems using liquid binders. Hapgood et al. (2003) presented and validated the regime map using lactose powders with two different size distributions and several different liquid binders. Ax et al. (2008) studied the effect of dimensionless spray flux by changing the droplet size and liquid flow rate on granule size and binder distribution where lactose

Table 2
Physical properties of gabapentin and HPC.

Properties	Gabapentin	HPC EXF	HPC EF
True density (g/cm^3)	1.2384 ± 0.0002	1.1897 ± 0.0002	1.1936 ± 0.0004
d_{10} (μm)	40.1 ± 8.9 (67)[a]	7.6 ± 0.2	168.1 ± 16.2
d_{50} (μm)	169.3 ± 5.2 (163)[a]	33.0 ± 1.1	422.5 ± 16.0
d_{90} (μm)	445.5 ± 70.6 (291)[a]	96.5 ± 3.1	822.8 ± 12.4

[a] The values in parenthesis are the results of sieve analysis, the rest are from laser diffraction analysis.

is used as the granulation material and water is used as the liquid binder. Hapgood et al. (2010) presented a pharmaceutical case study where the dimensionless spray flux is reduced to improve the liquid distribution for a multicomponent granulation material (API, microcrystalline cellulose, sodium starch glycolate, aluminium magnesium silicate). There have been no studies which test the Hapgood regime map approach (taking into account both drop penetration time and dimensional spray flux) using dry binders that are activated by the addition of a low viscosity solvent spray, e.g. water, which is a very common practice in industry. Some recent studies focused on granulation using only dry binders in order to understand the granulation mechanism and how granule properties are affected by dry binder properties (Herder et al., 2006; Larsson et al., 2008). Some workers have shown that dry amorphous binders can be activated if humidity causes the binder to drop below its glass transition temperature (Cavinato et al., 2010; Li et al., 2011; Palzer, 2009). This process is analogous to activation of a melt binder by increasing the temperature. In a typical high shear granulation with a dry binder, a low viscosity liquid is added from a spray which may then penetrate the bed by capillary action while simultaneously softening and partially dissolving the dry binder. This process is more complex than both the humidity driven activation described above and the capillary based models for drop penetration time given by Hapgood et al., 2002. Thus, the applicability of the simplified regime map approaches to more complex formulations needs further evaluation.

This paper focuses on testing the different regimes in the wet granulation nucleation regime map using a pharmaceutical formulation that constitutes Gabapentin and a dry binder (HPC) in a laboratory scale high shear granulator. We will examine the effect of process conditions and formulation properties on the nucleation regime of operation and use the information gathered from regime map to make predictions about the resulting granule size distribution. The applicability of the regime map approach to this more complex formulation will be critically assessed and the general applicability of the approach discussed.

2. Materials and methods

2.1. Materials and material characterization

The base formulation for this study consisted of gabapentin (Pfizer) with HPC (Hercules, Klucel EXF) used as the dry binder. The mass ratio of gabapentin to HPC was kept constant in all experiments at 15:1. De-ionized water was used as granulation liquid. All granulation studies used this formulation. For drop penetration time studies, experiments were also performed with a coarser grade of HPC (Hercules, Klucel EF) in the same mass ratio, and with pure gabapentin with no dry binder.

The particle size distribution of gabapentin was determined with both sieve analysis and laser diffraction method (Malvern Mastersizer 2000, Hydro S) (Fig. 1). The gabapentin supplied for this study has median particle size of 169.3 μm, which is larger than the materials that normally need to be granulated. Both HPC particle size distributions were measured by laser diffraction using a dry powder disperser (Malvern Mastersizer 2000, Scirocco 2000 M). Table 2 gives key size distribution and true density values for the powder materials. True density values were measured using a helium pycnometer (Micromeritics AccuPyc II 1340) after keeping samples in a dessicator for one week. Tapped density and bulk density were measured in a 100 mL graduated cylinder with a Varian Tapped Density Tester. Bulk and tapped densities are reported in Table 3 for pure gabapentin and for gabapentin plus HPC mixtures. Each measurement was repeated three times for all tests. The results are presented as mean values with 95% confident interval. Fig. 2 shows microscope images of

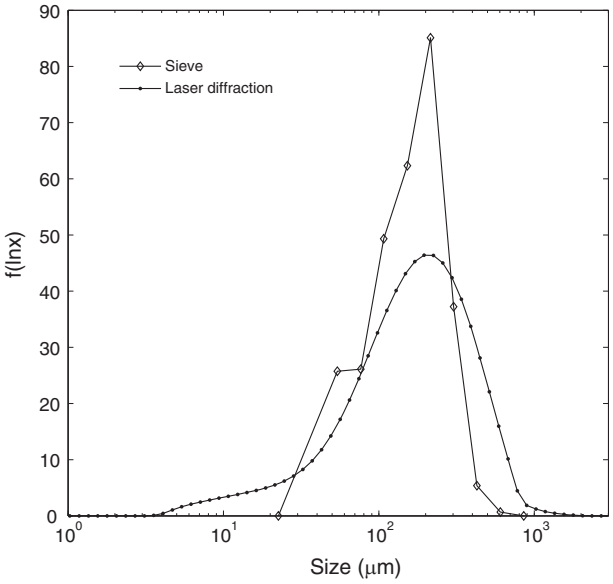

Fig. 1. Particle size distribution of gabapentin.

the gabapentin and HPC Klucel EFX (Nikon SMZ-1500 Stereoscopic Zoom Microscope).

Penetration time of liquid binder into the powder bed was measured as follows. Pure gabapentin, and premixed samples (15:1 gabapentin-Klucel EXF, 15:1 gabapentin-Klucel EF) were placed in a petri dish and the surface was leveled gently with a ruler without exerting force that could cause compaction. A drop of water was released onto the powder bed from a syringe. The distance between the powder bed and the needle tip was 5 cm. The course of penetration was recorded by a high speed camera (Photron, Fastcam-X 1024 PCI). Penetration time was determined by analyzing the videos. Drop penetration was judged to end when there was no significant change in the reflections seen on the granule nucleus. A twenty two gauge needle was used for drop penetration experiments giving a drop size of 2.80 ± 0.03 mm. From this measurement, the penetration time for any other drop size can be calculated from the following equation (Hapgood et al., 2002):

$$\frac{t_{p,1}}{t_{p,2}} = \frac{d_{d,1}^2}{d_{d,2}^2} \quad (5)$$

For each formulation, drop penetration time was taken as the average of 10 measurements.

2.2. Granulation experiments and process characterization

A Diosna P1-6 granulator with 6 L bowl was used for all granulation experiments. The bowl diameter was 25 cm and height was 14 cm. A batch size of 1.19 kg was used in all experiments. The loose bulk density of the gabapentin/HPC EXF mixture was measured as 0.57 ± 0.02 g/cm^3 and the corresponding volumetric fill fraction in the granulator was 35%.

To begin an experiment, the granulation material was dry mixed for 5 min at 500 rpm prior to water addition. The impeller speed was

Table 3
Physical properties of gabapentin and gabapentin–HPC mixtures.

	$d_{[3,2]}$ (μm)	Bulk density (g/cm^3)	Tapped density (g/cm^3)
Pure gabapentin	78.4	0.61 ± 0.02	0.83 ± 0.03
Gabapentin–HPC EF (15:1, w/w%)	81.8	0.59 ± 0.01	0.83 ± 0.01
Gabapentin–HPC EXF (15:1, w/w%)	61.3	0.57 ± 0.02	0.79 ± 0.03

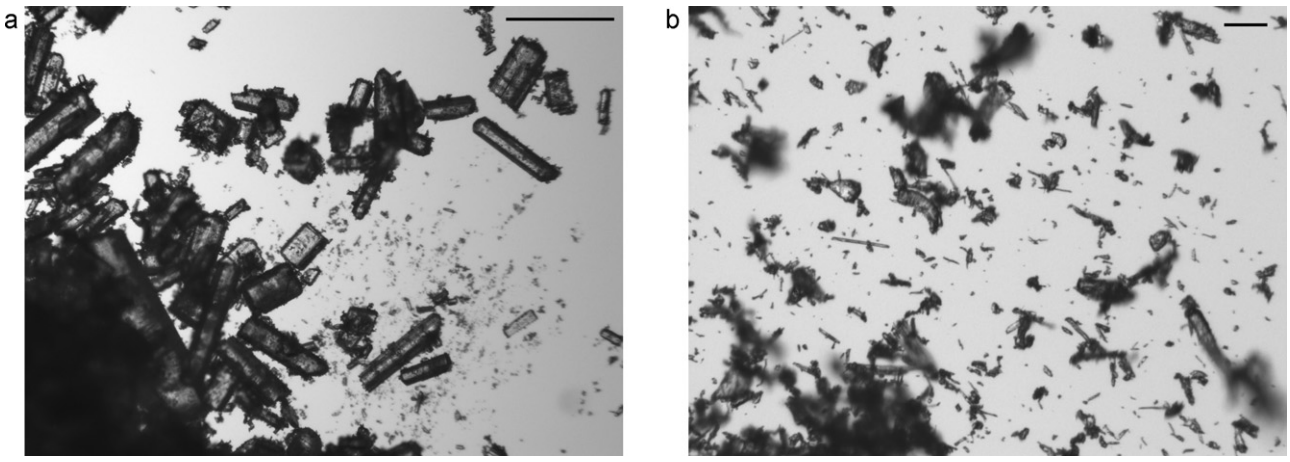

Fig. 2. Microscope images for (a) gabapentin (scale corresponds to 500 μm), and (b) HPC Klucel EFX (scale corresponds to 50 μm).

adjusted to that required for the experiment and water added by a spray nozzle or drip tube. The chopper speed was set to 1000 rpm for all experiments. The water addition time was set by the required spray rate and desired liquid content. Approximately 100 g of sample was taken from the granulator for size analysis after the liquid addition step. All the batches were then subject to 2 min of wet massing. After wet massing was completed, the final granules were removed and riffle split to yield a sample for size analysis. Granule samples for size analysis were tray dried overnight at 50 °C and at ambient humidity. The granule size distribution was then determined by sieve analysis using a $\sqrt{2}$ sieve series from 63 μm to 1 mm with material greater than 1 mm designated as "lumps". For d_{90} value calculations, the largest granule size was considered arbitrarily as 1400 μm. On the figures, the granule size distributions are presented as the normalized mass frequency of logarithm of particle size (Allen, 2003), where:

$$f(\ln x) = \frac{y_i}{\ln(x_i/x_{i-1})} \quad (6)$$

where y_i is the mass fraction in size interval i and x_i is the top size of size interval i.

To calculate the important dimensionless groups for regime map analysis, the liquid spray characteristics and powder surface velocity were measured. Water was introduced onto the powder bed either by spraying or in dripping mode. Two flat spray pattern nozzles with different volumetric capacities were used (Spraying Systems Co, 650017-SS and 650008-TP). Tygon 18 tubing (7.9 mm ID) was used to deliver the liquid in dripping mode. The lowest spray rate used in this study (29 g/min) was obtained with 650008-TP flat fan spraying nozzle at 40 psi. The distance between the tip of the nozzle and the powder surface and the angle of the nozzle were adjusted so that the spray width was 5 cm on the powder surface. A higher flow rate of 119 g/min was obtained with 650017-TP flat fan spraying nozzle at 100 psi. The width of this spray on the powder bed was 6 cm. The nozzle was located perpendicular to the powder flow and right before the chopper. The location of the nozzle was adjusted so that the liquid did not hit to the walls or to the impeller. No accumulation on the walls or on the impeller was observed after the experiments. Drop size distributions for both nozzles were analyzed 5 cm below the nozzle tip using Phase Doppler Analyzer (Dantec Dynamics, Skovlunde, Denmark, dual-PDA). The volume based median drop size produced by nozzles 650017-SS (at 100 psi) and 650008-TP (at 40 psi) were 72 μm and 93 μm, respectively. The drop size formed in dripping mode was calculated as 7 mm from the balance between the surface tension and gravitational forces.

The powder surface velocity was measured at 35% fill ratio and at 250 and 500 rpm impeller speeds using the high speed camera at 1000 frames/s. The camera was placed perpendicular to the powder surface capturing the flow near the wall. Especially at 500 rpm, dust blocked the visibility of the dry powder surface. Therefore, the powder surface velocities were measured after spraying 10 s of water at 29 g/min. The images from high speed videos were analyzed using image analysis software (GIMP) and dry agglomerates or cracks on the powder surface were tracked to measure surface velocity. Twelve spot measurements of surface velocities were taken for each impeller speed, 11 experiments were conducted varying impeller speed, mode of liquid addition (spray or drip), liquid flow rate and liquid level. A summary of all experiments undertaken is given in Table 4.

3. Results and discussion

3.1. Nucleation regime mapping

The nucleation process is a function of dimensionless spray flux and dimensionless drop penetration time. There are three regions defined on nucleation regime map (Fig. 3). To achieve good liquid distribution, and thus a narrow granule size distribution and a minimum of lump formation, operation should be in the drop controlled

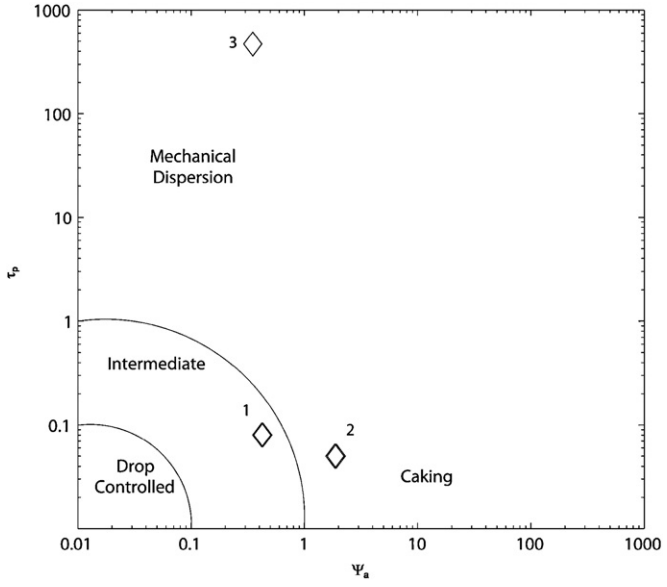

Fig. 3. Nucleation regime map and location of experimental conditions on the map.

Table 4
Summary of experimental conditions.

Run #	Liquid level[a] (%)	Impeller speed (rpm)	Liquid flow rate (g/min)	Spraying time (sec)	τ_p	ψ_a
1	2	250	29	49	0.08	0.43
2	2	500	29	49	0.08	0.42
3	2	250	119	12	0.05	1.91
4	2	500	119	12	0.05	1.86
5	4	250	29	99	0.08	0.43
6	4	500	29	99	0.08	0.42
7	4	250	119	24	0.05	1.91
8	4	500	119	24	0.05	1.86
9	4	250	245	12	471	0.35[b]
10	10	250	29	248	0.08	0.43
11	10	500	119	60	0.05	1.86

[a] The liquid levels are calculated based on total amount of dry powder used in granulation.
[b] Dripping mode.

regime with low dimensionless spray flux and low drop penetration time. Our objective is to test Hapgood's regime map approach for a broad size distribution formulation with a dry binder. Thus, we need to characterize the system parameters and design set of experiments where operation is (a) in the intermediate regime; (b) in the mechanical dispersion regime due to high spray flux; and (c) in the mechanical dispersion regime due to high drop penetration time. (b) and (c) are achieved by varying spray rate and drop size respectively. Experiments were performed at several liquid contents and at two impeller speeds to test the robustness of the nucleation regime map and for future studies on growth regime mapping. Table 4 lists the full experimental design.

Table 5 lists the measured drop penetration times for pure gabapentin, gabapentin plus Klucel EXF and gabapentin plus Klucel EF. The results are shown for the actual drop size during the penetration time experiment (2.80 ± 0.03 mm) and calculated using Eq. (5) for characteristic drop sizes during granulation experiments for the spray and dripping modes. The median drop size for the two spray nozzles used were measured as 93 and 72 μm respectively, while in dripping mode the drop size was 7 mm. Table 5 shows that the addition of a fine dry binder has a dramatic effect on the drop penetration time. Hapgood et al. (2002) showed that the drop penetration time (time needed for the drop fully penetrate into the powder bed after the initial impact) for simple systems can be related to powder and liquid properties by the following equations:

$$t_p = 1.35 \frac{{V_d}^{2/3}}{{\varepsilon_{eff}}^2 R_{eff}} \frac{\mu}{\gamma_{lv} \cos\theta} \quad (7)$$

where V_d is drop volume, μ is the liquid viscosity, and $\gamma_{lv} \cos\theta$ is the adhesive tension between the liquid and the powder. The effective powder bed porosity and effective pore size are given by:

$$\varepsilon_{eff} = \varepsilon_{tap}(1 - \varepsilon_b + \varepsilon_{tap}) \quad (8)$$

$$R_{eff} = \frac{\varphi d_{32}}{3} \frac{\varepsilon_{eff}}{1 - \varepsilon_{eff}} \quad (9)$$

where φ is the particle sphericity, d_{32} is the specific surface mean particle size, ε_b is loose packed bed porosity, and ε_{tap} is the tapped bed porosity. Effective bed porosity given in Eq. (8) takes into account the macrovoids in the powder bed which decrease the available pore volume for penetration. The details of derivation for both equation 8 and 9 can be found elsewhere (Hapgood et al., 2002).

Adding the fine dry binder will change the effective pore size and powder bed packing (Table 5). The effective pore sizes and effective pore radii were calculated for pure gabapentin and gabapentin HPC mixtures. The resultant values are used in Eq. (7) to calculate and compare the drop penetration time for different powder beds.

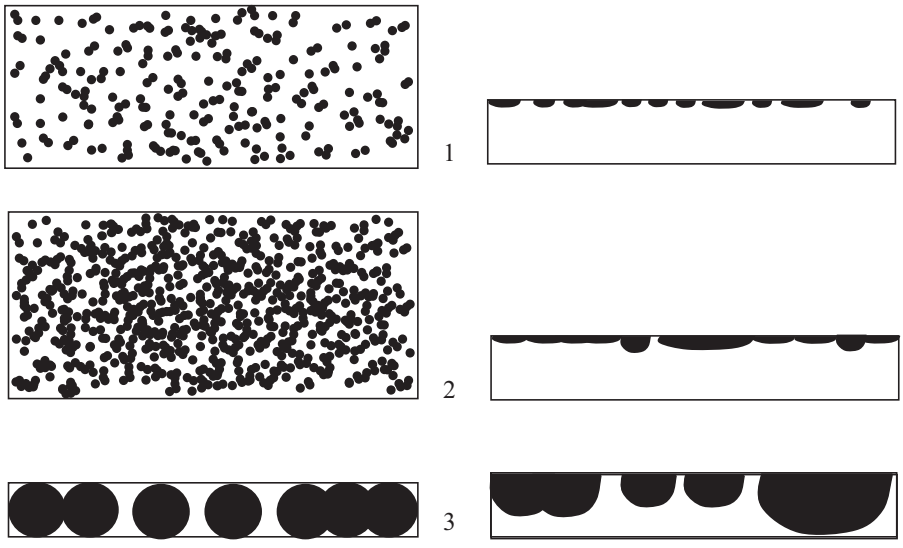

Fig. 4. Schematic representation of the spray zone for each point shown on nucleation map (in Fig. 3). 1: Intermediate region with spraying, ψ_a: 0.42–0.43; 2: Mechanical dispersion with spraying, ψ_a: 1.86–1.91; 3:Mechanical dispersion in dripping mode, ψ_a: 0.35. Left side: top view, right side: side view.

Table 5
Drop penetration time for different drop sizes.

	ε_{eff}	R_{eff}	Comparison of drop penetration time from Eq. (7)	Drop penetration time (s)			
				2.8 mm[a]	93 μm[b]	72 μm[b]	7 mm[b]
Pure Gabapentin	0.27	9.68	t_p	2.95 ± 0.30	0.003	0.002	18.4
Gabapentin–HPC EF (15:1, w/w%)	0.27	10.01	0.98 t_p	3.11 ± 0.25	0.003	0.002	19.4
Gabapentin–HPC EXF (15:1, w/w%)	0.30	9.01	0.90 t_p	75.44 ± 3.97	0.083	0.050	471.3

[a] Measured value.
[b] Calculated from Eq. (5).

When fine dry binder is added to gabapentin, the drop penetration time is expected to decrease slightly according to Eq. (7) (capillary penetration for simple systems). However, in reality, there is a 25-fold increase in drop penetration time (see Table 5). We hypothesize that the large increase in penetration time is partly due to plasticizing or partial solubilizing of the dry binder giving a barrier of highly viscous sticky material so that the effective liquid viscosity in the penetration time equation is very high. Note that this effect is maximized for the current formulation where most of the drug particles are coarse. The water drop is attracted to small pores by capillary action. The small pores are associated with small particles and therefore the dry binder. In contrast, there is little difference between the penetration time between the pure gabapentin and gabapentin with coarse dry binder. The effect on penetration time will be significant if the time scale for this process is similar to, or faster than that for capillary penetration. The time scale for plasticizing/solubilization binder will be proportional to the surface area of the powder and therefore decrease with decreasing dry binder particle size. Thus, the impact of the dry binder solubilization on penetration time is greatest when there is a large difference between the size distributions of the binder and especially when it is small compared to the rest of the formulation.

Nevertheless, when scaled to the drop size from the spray nozzle, the penetration times are at or near those required for drop controlled granulation (points 1 and 2 on Fig. 3). However, in dripping mode, the penetration times are very high and clearly in the mechanical dispersion regime (Point 3 on Fig. 3). [Note that drop penetration time measurement is relatively straightforward. However, determining the flow patterns inside the granulator, in order to measure the circulation time is difficult. The surface velocity of the powder bed was measured, and circulation time was estimated, from the surface velocity measurements. We estimated the circulation time between visits to the spray zone to be of order 1 s.]

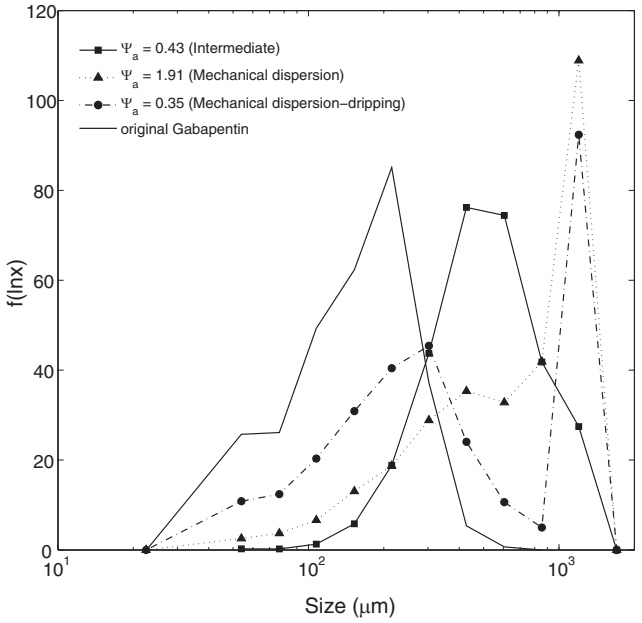

Fig. 5. Effect of dimensionless spray flux on particle size distribution of granules at 4% liquid content and 250 rpm impeller speed before wet massing (ψ_a: 0.42 corresponds to Point 1; ψ_a: 1.91 corresponds to Point 2; ψ_a: 0.35 corresponds to Point 3 in Figs. 3 and 4).

The dimensionless spray flux by definition determines the density of the liquid binder droplets hitting on the powder surface through the spray zone. To calculate the dimensionless spray flux, powder surface velocities are required. The mean powder surface velocities at 250 rpm and at 500 rpm were found to be 0.36 ± 0.04 m/s and 0.37 ± 0.03 m/s respectively. The impeller tip speeds at 250 and 500 rpm are 3.27 and 6.54 m/s, respectively. The powder surface velocities are approximately an order of magnitude smaller than the tip speeds. The powder flows in roping regime at both impeller speeds. As previously shown in the literature (Litster et al., 2002; Ramaker et al., 1998), impeller speed does not have significant effect on the powder surface velocity in the roping regime. With the surface velocity measurement and knowledge of the spray geometry, spray rate and drop size, the dimensionless spray flux can be calculated using Eq. (1). Table 4 shows the lower spray rates gave ψ_a values, ranging between 0.42 and 0.43 (intermediate region, Point 1 on Fig. 3), whereas high spray rates gave higher ψ_a values, 1.86 and 1.91 (mechanical dispersion regime, Point 2 on Fig. 3). We were not able to achieve low enough spray fluxes for the drop controlled regime with the available nozzles. At lower spray rates, the nozzles began to drip.

In dripping mode, the spray flux is calculated by taking the drop diameter as the spray width. For the dripping condition, the spray flux is calculated as 0.35(mechanical dispersion regime, Point 3 on Fig. 3). The flow of water, pumped with a peristaltic pump, was investigated by high speed camera and it was observed that there is flow approximately for 0.1 sec and then there is a pause for 0.2 sec. These flow and pause events are periodic. Thus the instantaneous spray flux is higher than 0.35. However, intermittent nature of the flow might be allowing time for breakup of the lumps before new ones are formed.

3.2. Predicting granulation behavior from the regime map

None of the available experimental conditions were in the drop controlled regime (see Fig. 3). When the sprays were used, the dimensionless drop penetration time was estimated as 0.08 and 0.05 for drop sizes of 93 μm and 72 μm, respectively. Although the drop penetration time values were low enough to be in the drop controlled regime, the region of operation was either in intermediate region or in the mechanical dispersion region due to the spray rates. The spray rate of 29 g/min provides experimental conditions to operate in the intermediate region and the spraying rate of 119 g/min resulted in mechanical dispersion region (Fig. 3). The dimensionless drop penetration time for dripping mode is estimated as 471, which well into the mechanical dispersion

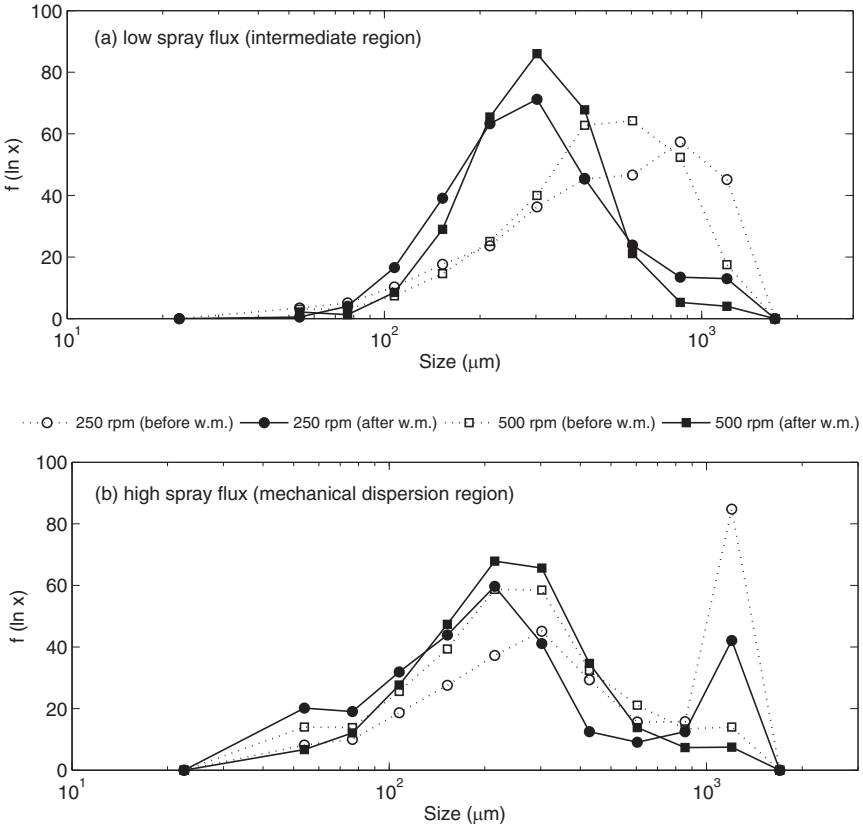

Fig. 6. Granule size distributions before and after wet massing for 2% liquid content (a) at low spray flux (Point 1 in Figs. 3 and 4), (b) at high spray flux (Point 2 in Figs. 3 and 4).

regime independent of the value of the dimensionless spray flux.

As none of the experiments was in the drop controlled regime, we expect some lump formation in all experiments. However, the fewest lumps and the narrowest granule size distribution should occur for experiments conducted in the intermediate regime, i.e. using the spray nozzle with low spray rate (Point 1 on Fig. 3). Point 2 is in the mechanical dispersion regime mainly due to the high spray rate but the drop size and drop penetration time are relatively small. The drops will form a thin layer of caked surface on the powder bed which is expected to cause wider size distribution and higher percentage of lumps compared to Point 1 (see Fig. 4). Point 3 is also in the mechanical dispersion regime. However, at Point 3, the drop penetration time is 9448 times larger than it is at Point 2 due to the 97.2 times difference in drop size. Pooling of liquid on the powder surface may occur and the size of the lumps will be larger (Fig. 4). The breakup of the thinner caked surface is easier by mechanical dispersion than the breakup of larger sticky lumps. Therefore at Point 2, the liquid distribution would be better compared to Point 3. Therefore we expect the largest number of lumps and the broadest granule size distribution at Point 3.

We expect that the qualitative trends described above to be true at all wet massing times, impeller speeds and liquid contents, especially with regard to the presence of lumps. However, as the granulation proceeds, granule consolidation, growth and breakage will lead to changes in the mean granule size and the granule size distribution.

In summary, the expectations of the granule size distribution based on the nucleation regime map are:

- Lump formation is expected at all conditions due to the nature of the formulation and limitations on the minimum spray rate from the nozzles, but more lumps are expected when operating in mechanical dispersion region.
- The narrowest distribution and widest distributions are expected for Points 1 and 3, respectively.
- At a particular liquid content, as the impeller speed increases, the dimensionless spray flux does not change significantly since the powder surface velocity does not change. However, changing the impeller speed may affect the breakage of lumps and smaller amount of lumps are expected at higher impeller speeds.
- The qualitative predictions about the granule size distributions are expected to be most obvious at lower liquid contents, where the nucleation process dominates over granule growth.

3.3. Experimental granulation results

Table 6 shows median size, span, and the percentage of the lumps (+1 mm granules) obtained in each experiment before wet massing. Fig. 5 shows the full granule size distributions at 4% liquid content at high and low spray flux and for water addition by dripping at 250 rpm impeller speed. As the spray flux increases from Point 1 (ψ_a = 0.42 and 0.43) to Point 2 (ψ_a = 1.86 and 1.91) on the regime map (i.e. moving the operating point from the intermediate regime to mechanical dispersion), there is an increase in the amount of lumps and an increase in the amount of fines leading to a broadening of the size distribution. The broadest distribution was obtained for Point 3 (mechanical dispersion-dripping), where there is clearly very poor liquid distribution with a large proportion of both lumps and ungranulated powder. Very poor liquid distribution in the mechanical dispersion regime is supported by the bimodal distribution (Fig. 5). At all conditions, some lumps are found, reflecting that none of the operating conditions fall within the drop controlled regime. The amount of lumps varies greatly with operating conditions and, in

Table 6
Characteristics of granule size distributions before wet massing.

Run #[a]	Fluid level (%)	Impeller speed (rpm)	ψ	τ_p	d_{10} (μm)	d_{90} (μm)	d_{50} (μm)	+1 mm granules (%)
1 (P1)	2	250	0.43	0.08	156	1137	515	15.2
2 (P1)	2	500	0.42	0.08	181	934	475	5.9
3 (P2)	2	250	1.91	0.05	111	1260	351	28.5
4 (P2)	2	500	1.86	0.05	91	690	244	4.7
5 (P1)	4	250	0.43	0.08	252	1067	537	12.0
6 (P1)	4	500	0.42	0.08	263	1045	610	11.3
7 (P2)	4	250	1.91	0.05	190	1291	730	36.6
8 (P2)	4	500	1.86	0.05	235	994	568	9.5
9 (P3)	4	250	0.35 (dripping)	471	100	1271	320	31.1
10 (P1)	10	250	0.43	0.08	476	+1000	+1000	56.3
11 (P2)	10	500	1.42	0.05	595	+1000	+1000	77.2

[a] The values in parenthesis show the location of the experiment on the nucleation regime map (Refer Fig. 3). P1: Point 1 (intermediate regime), P2: Point 2 (mechanical dispersion regime with spraying), P3: Point 3 (mechanical dispersion regime in dripping mode).

general, is highest for experiments in the mechanical dispersion regime.

At any specific liquid content, the median granule size decreases only slightly as the the spray flux moves from intermediate region to mechanical dispersion region (from Point 1 to Point 2) with an exception at 4% liquid content and low impeller speed. However, the amount of lumps increases dramatically with increased spray flux at the low impeller speed.

The powder flow during granulation is in roping regime at 250 rpm and 500 rpm providing good turnover at both cases. For both 2% and 4% liquid content, increasing the impeller speed gives narrower size distributions and reduces the proportion of large lumps. At higher impeller speed, there is a greater rate of breakage of lumps. Although, the surface velocity is nearly independent of the impeller speed in roping regime, the maximum impact velocity in the impeller zone is doubled at 500 rpm increasing the probability of lump breakage (Liu et al., 2009). The effect of impeller speed is more dramatic at high spray flux because of the increased lump formation in the mechanical dispersion regime, e.g. at 2% liquid content, the decrease in the amount of lumps when impeller speed was increased was from 15.2% to 5.9% at lower spray flux and from 28.5% to 4.7%at high spray flux. Note, however, that some lumps persist even at the higher impeller speeds. Operating at low spray flux is the best way to keep the granule size distribution narrow.

At 10% liquid content, the majority of the granule size distribution is greater than 1 mm under all conditions due to rapid granule growth.

Table 7 shows a summary of the granule size distribution parameters under all conditions after 2 min wet massing time. Lumps are still seen under all experimental conditions and, in general, operating in the intermediate regime leads to less lump formation and narrower granule size distributions. However, the change in granule size distribution with wet massing will depend on the balance between lump breakage and granule growth which varies according to the experimental conditions. Fig. 6 and 7 show the granule size distributions before and after wet massing for 2% and 4% liquid contents, respectively. Table 8 summarizes the changes in the characteristics of granule size distributions after wet massing.

At 2% liquid content, the granule size distribution is dominated by nucleation and there is little or no granule growth. Wet massing induces the breakage of the lumps at all impeller speeds and spray fluxes (Tables 7 and 8, Fig. 6). At the lower spray flux, 71.1% and 76.3% of the initial lumps are broken at 250 and 500 rpm, respectively (Table 8). At the higher spray flux, 50.2% and 46.8% of the initial lumps are broken at 250 and 500 rpm, respectively. These results indicate that more lumps can be broken at the lower spray flux irrespective of the impeller speed. The breakage effect can be also seen on d_{50} values. The d_{50} values are almost halved (Table 8) except high spray flux-high impeller speed after wet massing. The granule size distributions shifted left after wet massing, which indicates the dominating effect of granule breakage (Fig. 6).

At 4% and 10% liquid content, wet massing had little effect on the granule size distribution under most conditions (Fig. 7, Table 8). There is evidence of a small amount of granule growth at 500 rpm but not at 250 rpm. At 250 rpm, the granule size distribution is either unchanged, or there is a decrease in the proportion of lumps due to breakage (4%, 250 rpm, high spray flux).

Ax et al. (2008) studied lactose granulation with water in the intensive mixer Eirich R02 that consists of a rotating vessel, a mixing tool, and a wall scraper. They found that when the liquid is sprayed, smaller nozzles (lower dimensionless spray flux) provide better liquid distribution. They also stated that pouring the water compared to spraying at the same flow rate results in a broader

Table 7
Characteristics of granule size distributions after wet massing.

Run #[a]	Fluid level (%)	Impeller speed (rpm)	ψ	τ_p	d_{10} (μm)	d_{90} (μm)	d_{50} (μm)	+1 mm granules (%)
1 (P1)	2	250	0.43	0.08	136	684	283	4.4
2 (P1)	2	500	0.42	0.08	156	516	299	1.4
3 (P2)	2	250	1.91	0.05	76	1118	215	14.2
4 (P2)	2	500	1.86	0.05	103	499	234	2.5
5 (P1)	4	250	0.43	0.08	258	985	498	9.2
6 (P1)	4	500	0.42	0.08	284	1224	671	22.7
7 (P2)	4	250	1.91	0.05	214	1138	449	15.3
8 (P2)	4	500	1.86	0.05	261	1121	596	14.3
9 (P3)	4	250	0.35 (dripping)	471	95	1261	282	28.8
10 (P1)	10	250	0.43	0.08	554	+1000	+1000	55.8
11 (P2)	10	500	1.42	0.05	960	+1000	+1000	89.2

[a] The values in parenthesis show the location of the experiment on the nucleation regime map (refer Fig. 3). P1: Point 1 (intermediate regime), P2: Point 2 (mechanical dispersion regime with spraying), P3: Point 3 (mechanical dispersion regime in dripping mode).

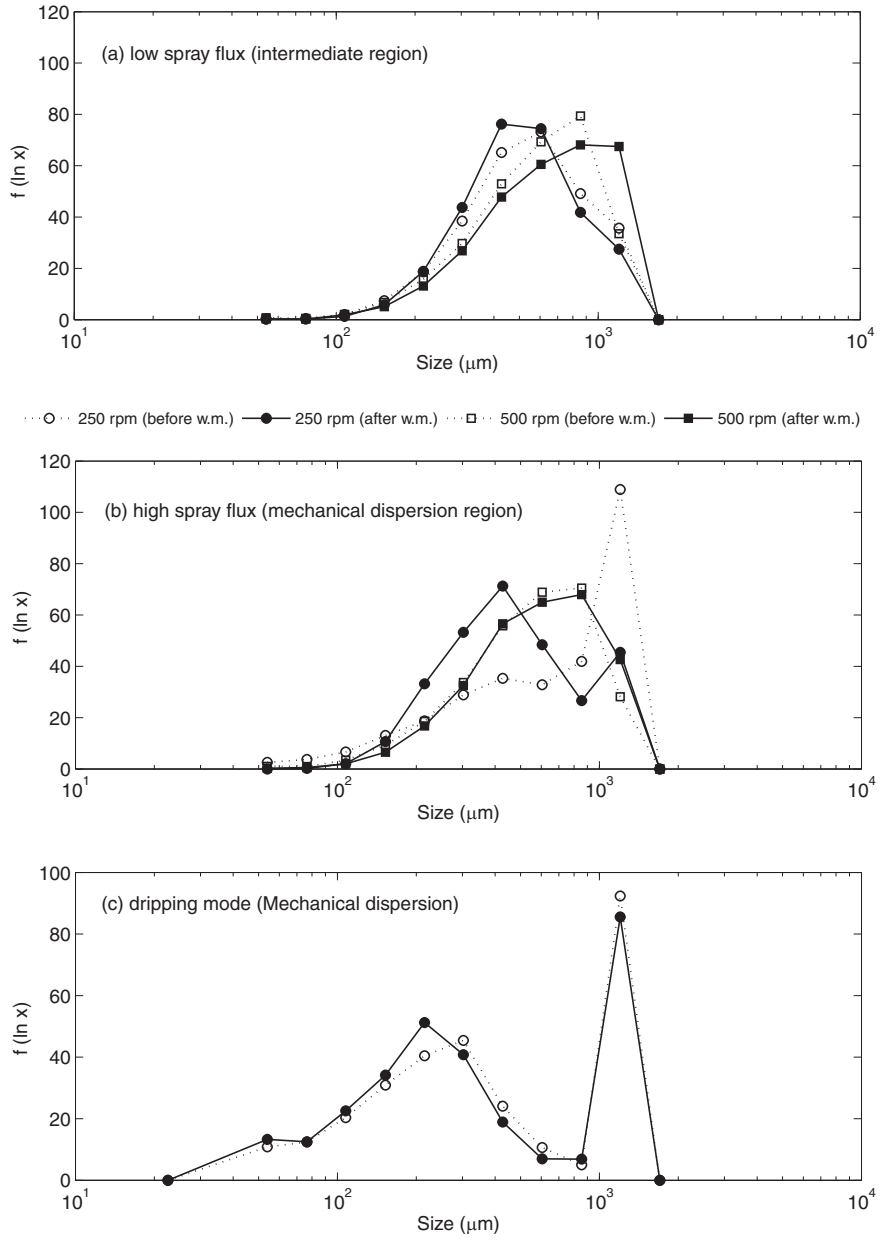

Fig. 7. Granule size distributions before and after wet massing for 4% liquid content (a) low spray flux (Point 1 in Figs. 3 and 4), (b) high spray flux (Point 2 in Figs. 3 and 4), (c) dripping mode (Point 3 in Figs. 3 and 4).

Table 8
Relative change in characteristics of granule size distributions after wet massing.

Run #[a]	Fluid level (%)	Impeller speed (rpm)	Δd_{10}[b] (%)	Δd_{90}[b] (%)	Δd_{50}[b] (%)	Δ+1 mm granules[b] (%)
1 (P1)	2	250	−12.8	−39.8	−45.0	−71.1
2 (P1)	2	500	−13.8	−44.8	−37.1	−76.3
3 (P2)	2	250	−31.5	−11.3	−38.7	−50.2
4 (P2)	2	500	13.2	−27.7	−4.1	−46.8
5 (P1)	4	250	2.4	−7.7	−7.3	−23.3
6 (P1)	4	500	8.0	17.1	10.0	100.9
7 (P2)	4	250	12.6	−11.9	−38.5	−58.2
8 (P2)	4	500	11.1	12.8	4.9	50.5
9 (P3)	4	250	−5.0	−0.8	−11.9	−7.4
10 (P1)	10	250	16.4	–	–	−0.9
11 (P2)	10	500	61.3	–	–	15.5

[a] The values in parenthesis show the location of the experiment on the nucleation regime map (Refer Fig. 3). P1: Point 1 (intermediate regime), P2: Point 2 (mechanical dispersion regime with spraying), P3: Point 3 (mechanical dispersion regime in dripping mode).

[b] The relative changes are calculated by $((\text{value}_{\text{after wet massing}} - \text{value}_{\text{before wet massing}})/\text{value}_{\text{before wet massing}}) \times 100$. For Δd_{10}, Δd_{50}, and Δd_{90}, the values used in the equation are in microns; for +1 mm granules the values used in the equation are the mass percentages.

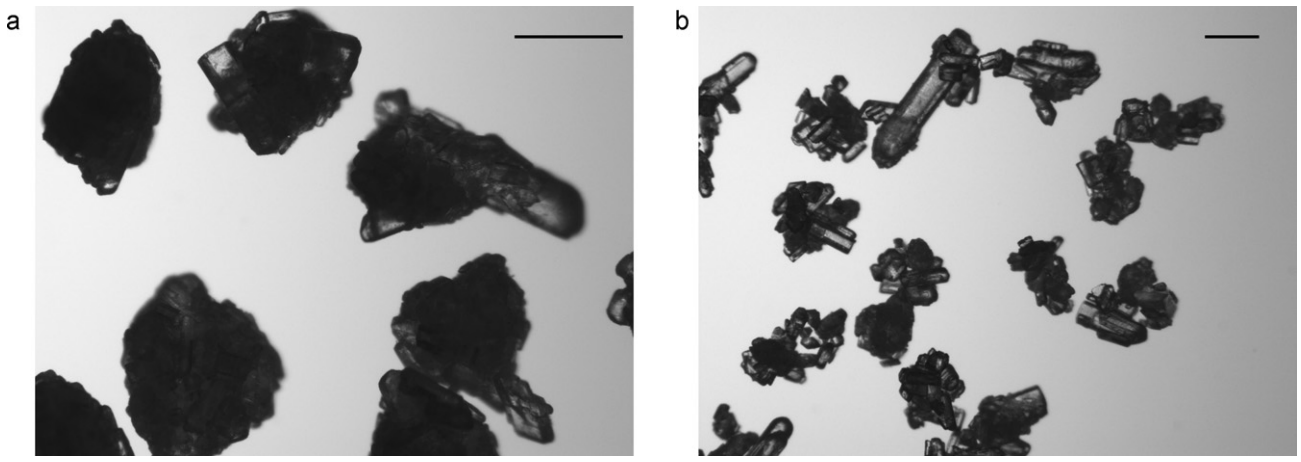

Fig. 8. Microscope images of granules from sieve cut +500 μm and −710 μm. (a) Run 1, (b) Run 5. Scales on both images correspond to 500 μm.

granule size distribution. These results are in agreement with the results presented in this study. However, they did not see significant difference between the particle size distributions of granules produced using different nozzles and also pouring method after 5 min of wet massing. In this study, even after wet massing time of 2 min, the difference in granule size distributions between different spray fluxes persists. This might be due to the difference in granulator type (the granulator designs in these studies are very different) or formulation or both.

Examination of microscope images of granules showed two types of granule structure (Fig. 8). One group of granules is, mostly composed of small particles and viscous HPC water solution (Fig. 8a). Sometimes, large gabapentin crystals are integrated into the granules. The second group exhibits a more open structure and are formed by either smaller particles sticking onto larger crystals or larger crystals forming a loose matrix (Fig. 8b). In this type of structure, individual crystals can be clearly seen. Both types of granule structure are seen at all liquid contents. However at 2% liquid content, larger granules (>500 μm) are mostly formed from fine particles whereas at 4% liquid content, 500 μm and larger size ranges have both types of granules. At 2% liquid content, mostly 90 μm and smaller particles are granulated. When the liquid content is increased, as more liquid becomes available for growth, larger particles start to form granules.

The liquid amount needed for the formulation of interest was very low. This may be due to two reasons: (1) the wide particle size distribution of original gabapentin where only smaller amount of the material needs to be granulated; and (2) inclusion of a dry binder which also acts as additional amount of liquid as it is activated. Determination of amount of liquid needed is important in order to determine end point for the process. In order to predict *a priori* how much liquid is needed for granulation, the growth regime map should be utilized. However, calculation of maximum saturation value is not straightforward for complex systems such as this one. Testing and validation studies of the growth regime map for formulations with dry binders are ongoing.

4. Conclusions

The main conclusions from the study are:

1. The addition of dry binder increases the drop penetration time in a way that could not be predicted from simple capillary flow considerations. For systems containing a dry binder or other amorphous powders, it is recommended that drop penetration time be measured directly for the blended formulation and then scaled to the drop size during spraying.
2. The effect of process conditions on the quality of the granule size distribution as measured by lump formation and the span of the size distribution was successfully predicted *a priori* using Hapgood's regime map analysis for the range of conditions studied. Wider granule size distributions and higher amount of lumps were obtained moving from intermediate to mechanical dispersion regime. Addition of the liquid in the dripping mode gave the broadest size distribution with ungranulated fines and highest percentage of lumps compared to spraying mode. Addition of the liquid by spraying in the intermediate regime gave the narrowest size distribution with the lowest amount of lumps.
3. The optimum liquid content for this formulation was 4%. This low value is due to a combination of the breadth of the initial particle size distribution and the activation of the dry binder during granulation.
4. The effects of impeller speed and wet massing time on granule size distribution were complex due to a balance between increased breakage of lumps and increased granule consolidation and growth. *A priori* prediction of the effect of liquid content, impeller speed and wet massing time requires a quantitative analysis for the growth and breakage regimes which is beyond the scope of this paper.

Acknowledgements

Financial support to this project is given by Food and Drug Administration (FDA) through the project HHSF223200819929C held by The National Institute of Pharmaceutical Technology and Education (NIPTE). The authors would like to thank Dr. Ariel Muliadi for the spray drop size measurements and Mauro Cavinato for his help during powder surface velocity measurements.

References

Adetayo, A.A., Ennis, B.J., 1997. Unifying approach to modeling granule coalescence mechanisms. AIChE J. 43, 927–934.
Allen, T., 2003. Powder Sampling and Particle Size Determination, first ed. Elsevier B.V., Amsterdam, The Netherlands.
Ax, K., Feise, H., Sochon, R., Hounslow, M., Salman, A., 2008. Influence of liquid binder dispersion on agglomeration in an intensive mixer. Powder Technol. 179, 190–194.
Benali, M., Gerbaud, V., Hemati, M., 2009. Effect of operating conditions and physicochemical properties on the wet granulation kinetics in high shear mixer. Powder Technol. 190, 160–169.
Biggs, C.A., Sanders, C., Scott, A.C., Willemse, A.W., Hoffman, A.C., Instone, T., Salman, A.D., Hounslow, M.J., 2003. Coupling granule property and granulation rates in high-shear granulation. Powder Technol. 130, 162–168.

Bouwman, A.M., Henstra, M.J., Westerman, D., Chung, J.T., Zhang, Z., Ingram, A., Seville, J.P.K., Frijlink, H.W., 2005. The effect of the amount of binder liquid on the granulation mechanisms and structure of microcrystalline cellulose granules prepared by high shear granulation. Int. J. Pharm. 290, 129–136.

Bouwman, A.M., Visser, M.R., Meesters, G.M.H., Frijlink, H.W., 2006. The use of Stokes deformation number as a predictive tool for material exchange behaviour of granules in the "equilibrium phase" in high shear granulation. Int. J. Pharm. 318, 78–85.

Cantor, S.L., Kothari, S., Koo, O.M.Y., 2009. Evaluation of the physical and mechanical properties of high drug load formulations: wet granulation vs. novel foam granulation. Powder Technol. 195, 15–24.

Cavinato, M., Bresciani, M., Machin, M., Bellazzi, G., Canu, P., Santomaso, A.C., 2010. Formulation design for optimal high-shear wet granulation using on-line torque measurements. Int. J. Pharm. 387, 48–55.

Freireich, B., Li, J., Litster, J., Wassgren, C. Incorporating particle flow information from discrete element simulations in population balance models of mixer-coaters. Chem. Eng. Sci., in press.

Gantt, J.A., Gatzke, E.P., 2005. High-shear granulation modeling using a discrete element simulation approach. Powder Technol. 156, 195–212.

Ghorab, M.K., Adeyeye, M.C., 2007. High shear mixing granulation of ibuprofen and β-cyclodextrin: effects of process variables on ibuprofen dissolution. AAPS PharmSciTech 8, E1–E9.

Gokhale, R., Sun, Y., Shukla, A.J., 2005. High-shear granulation. In: Parikh, D.M. (Ed.), Handbook of Pharmaceutical Granulation Technology. Taylor and Francis Group, Boca Raton, FL, pp. 191–228.

Hapgood, K.P., Litster, J.D., Biggs, S.R., Howes, T., 2002. Drop penetration into porous powder beds. J. Colloid Interface Sci. 253, 353–366.

Hapgood, K.P., Litster, J.D., Smith, R., 2003. Nucleation regime map for liquid bound granules. AIChE J. 49, 350–361.

Hapgood, K.P., Amelia, R., Zaman, M.B., Merrett, B.K., Leslie, P., 2010. Improving liquid distribution by reducing dimensionless spray flux in wet granulation – A pharmaceutical manufacturing case study. Chem. Eng. J. 164, 340–349.

Herder, J., Adolfsson, A., Larsson, A., 2006. Initial studies of water granulation of eight grades of hypromellose (HPMC). Int. J. Pharm. 313, 57–65.

Hounslow, M.J., Pearson, J.M.K., Instone, T., 2001. Tracer studies of high-shear granulation: II. Population balance modeling. AIChE J. 47, 1984–1999.

Iveson, S.M., Litster, J.D., 1998. Growth regime map for liquid bound granules. AIChE J. 44, 1510–1518.

Iveson, S.M., Wauters, P.A.L., Forrest, S., Litster, J.D., Meesters, G.M.H., Scarlett, B., 2001. Growth regime map for liquid bound granules: further developments and experimental validation. Powder Technol. 117, 83–87.

Iveson, S.M., 2002. Limitations of one-dimensional population balance models of wet granulation processes. Powder Technol. 124, 219–229.

Kristensen, H.G., Schaefer, T., 1987. Granulation. A review on pharmaceutical wet-granulation. Drug. Dev. Ind. Pharm. 13, 803–872.

Larsson, A., Vogt, M.H., Herder, J., Luukkonen, P., 2008. Novel mechanistic description of the water granulation process for hydrophilic polymers. Powder Technol. 188, 139–146.

Le, P.K., Avontuur, P., Hounslow, M.J., Salman, A.D., 2011. A microscopic study of granulation mechanisms and their effect on granule properties. Powder Technol. 206, 18–24.

Li, L., Tao, L., Dali, M., Buckley, D., Gao, J., Hubert, M., 2011. The effect of the physical states of binders on high-shear wet granulation and granule properties: a mechanistic approach toward understanding high-shear wet granulation process. Part II. Granulation and granule properties. J. Pharm. Sci. 100, 294–310.

Liu, L.X., Smith, R., Litster, J.D., 2009. Wet granule breakage in a breakage only high-hear mixer: effect of formulation properties on breakage behavior. Powder Technol. 189, 158–164.

Litster, J.D., Hapgood, K.P., Michaels, J.N., Sims, A., Roberts, M., Kameneni, S.K., 2002. Scale-up of mixer granulators for effective liquid distribution. Powder Technol. 124, 272–280.

Mackaplow, M.B., Rosen, L.A., Michaels, J.N., 2000. Effect of primary particle size on granule growth and endpoint determination in high-shear wet granulation. Powder Technol. 108, 32–45.

Mangwandi, C., Adams, M.J., Hounslow, M.J., Salman, A.D., 2010. Effect of impeller speed on mechanical and dissolution properties of high-shear granules. Chem. Eng. J. 164, 305–315.

Mangwandi, C., Adams, M.J., Hounslow, M.J., Salman, A.D., 2011. Effect of batch size on mechanical properties of granules in high shear granulation. Powder Technol. 206, 44–52.

Michaels, J.N., Farber, L., Wong, G.S., Hapgood, K., Heidel, S.J., Farabaugh, J., Chou, J.-H., Tardos, G.I., 2009. Steady states in granulation of pharmaceutical powders with application to scale-up. Powder Technol. 189, 295–303.

Palzer, S., 2009. Influence of material properties on the agglomeration of water-soluble amorphous particles. Powder Technol. 189, 318–326.

Poon, J.M.-H., Immanuel, C.D., Doyle, F.J., Litster, J.D., 2008. A three dimensional population balance of granulation with a mechanistic representation of nucleation and aggregation phenomena. Chem. Eng. Sci. 63, 1315–1329.

Ramachandran, R., Immanuel, C.D., Stepanek, F., Litster, J.D., Doyle III, F.J., 2009. A mechanistic model for breakage in population balances of granulation: theoretical kernel development and experimental validation. Chem. Eng. Res. Des. 87, 598–614.

Ramaker, J.S., Jelgersma, M.A., Vonk, P., Kossen, N.W.F., 1998. Scale-down of a high shear pelletisation process: flow profile and growth kinetics. Int. J. Pharm. 166, 89–97.

Realpe, A., Velazquez, C., 2008. Growth kinetics and mechanism of wet granulation in a laboratory-scale high shear mixer: effect of initial polydispersity of particle size. Chem. Eng. Sci. 63, 1602–1611.

Smirani-Khayati, N., Falk, V., Bardin-Monnier, N., Marchal-Heussler, L., 2009. Binder liquid distribution during granulation process and its relationship to granule size distribution. Powder Technol. 195, 105–112.

Tardos, G.I., Irfan Khan, M., Mort, P.R., 1997. Critical parameters and limiting conditions in binder granulation of fine powder. Powder Technol. 94, 245–258.

Van den Dries, K., De Vegt, O.M., Girard, V., Vromans, H., 2003. Granule breakage phenomena in a high shear mixer; influence of process and formulation variables and consequences on granule homogeneity. Powder Technol. 133, 228–236.

Verkoeijin, D., Pouw, G.A., Meesters, G.M.H., Scarlett, B., 2002. Population balances for particulate processes – a volume approach. Chem. Eng. Sci. 57, 2287–2303.